ELSEVIER

Journal of Chromatography A, 725 (1996) 295–314

JOURNAL OF CHROMATOGRAPHY A

Optimization of preparative ion-exchange chromatography of proteins: linear gradient separations

S.R. Gallant, S. Vunnum, S.M. Cramer*

Isermann Department of Chemical Engineering, Rensselaer Polytechnic Institute, Troy, NY 12180, USA

Received 1 March 1995; revised 17 August 1995; accepted 17 August 1995

Abstract

In this study, the Steric Mass Action (SMA) model of ion exchange is employed in concert with appropriate mass balance equations to predict the separation performance of preparative ion-exchange chromatography. The model is able to accurately predict linear gradient separations of the proteins α-chymotrypsinogen A, cytochrome c, and lysozyme under overloaded conditions. The optimization behavior of preparative ion-exchange chromatography is examined under conditions of baseline resolution and induced sample displacement. This work demonstrates that a simple iterative procedure can be employed to establish optimal gradient conditions for preparative ion-exchange chromatography of proteins. The results also indicate that under appropriate conditions, sample displacement can be employed to dramatically improve the production rate with minor losses in product yield or purity. Linear gradient separations with sample displacement are also less sensitive to the adsorption properties of the feed stream than baseline resolved separations, resulting in simplified methods development.

Keywords: Steric mass action model; Preparative chromatography; Linear gradient separations; Ion exchange; Gradient elution; Optimization; Proteins

1. Introduction

In ion-exchange chromatography of proteins, gradient elution chromatography is commonly employed to separate feed streams which have components characterized by a wide range of chromatographic affinity. In linear gradient chromatography, a feed injection containing a low concentration of salt is applied to the column, and subsequently a ramp of increasing mobile phase salt is introduced into the column. This technique allows the proteins to be concentrated during the feed stage and subsequently eluted without substantial dilution.

The linear solvent strength theory of Snyder and Stadalius [1] allows retention to be predicted in the linear or Henry's law region of a single component isotherm. This theory has found widespread acceptance ([2,3] and Appendix) and has been extended to include contributions of various mass transport resistances to observed band broadening [4–6]. However, modeling of gradient elution represents a difficult challenge that cannot be met solely by analytical solutions of the equations of chromatography. The high concentrations which may be reached inside the column during the feed stage result in multicomponent competitive binding, implying that prediction of retention will require the use of numerical techniques [7–13].

*Corresponding author.

0021-9673/96/$15.00
SSDI 0021-9673(95)00909-4

Significant progress has been made in the understanding of protein separations by linear continuous and step gradient chromatography [2,7,8]. However, a lack of appropriate models of multicomponent protein adsorption has made it difficult to reconcile experimental and theoretical results under conditions of high protein concentration. Recently, the Steric Mass Action (SMA) model has made it possible to represent multicomponent competitive protein adsorption in ion-exchange chromatography over a range of salt concentrations [14,15]. SMA models protein adsorption in ion-exchange chromatography as a stoichiometric exchange [16,17]. Stoichiometric exchange or displacement has been utilized by Drager and Regnier to model protein adsorption under conditions of infinite dilution [18]. At higher protein concentrations, the finite capacity of the stationary phase [19] and the blockage or steric shielding of the stationary phase surface by biopolymers play important roles in equilibrium adsorption. Whitley et al. have developed a method for addressing the steric shielding phenomena in binding of a single protein at high concentration [20]. Li and Pinto have developed a method for addressing non-ideal protein adsorption based on UNIQUAC [21]. Significantly, Velayudhan observed that the number of blocked sites is proportional to the adsorbed protein concentration [22]. Brooks and Cramer used this insight as the basis of the SMA formalism [14].

Subsequently, SMA has been shown capable of representing the linear and nonlinear adsorption of proteins and polyelectrolytes over a range of mobile phase salt conditions [23]. Further, it has been successfully employed to represent nonlinear multicomponent adsorption occurring in displacement chromatography [24–26]. Recently, SMA based models have been used to predict the transient development process of displacement chromatography [27], to represent the adsorption equilibrium in nonlinear isocratic chromatography [15], and to predict the behavior of preparative step gradient chromatography [28].

In this paper, the SMA model will be employed in concert with appropriate mass transport equations and boundary conditions to describe linear gradient chromatography. This model will be used to gain greater insight in the optimization of linear gradient chromatography.

2. Theory

2.1. Chromatographic optimization

Optimization of preparative chromatographic systems must consider four types of variables: objective function, parameters, decision variables, and constraints. For the problem of optimization of a preparative separation by a linear gradient chromatography, the optimization variables are listed in Table 1 and will be discussed below.

2.1.1. Objective function

Optimization consists of maximization of an objective function. For preparative chromatography, that objective function may be taken to be the production rate of the process:

$$PR_i = \frac{C_{i,\mathrm{f}} V_\mathrm{f} Y_i}{t_\mathrm{cyc} V_\mathrm{sp}} \tag{1}$$

where $C_{i,\mathrm{f}}$ is the feed concentration of the i^{th} component, V_f is the feed volume, Y_i is the yield, t_cyc is the cycle time, and V_sp is the stationary phase volume. The numerator represents the mass of protein purified in a single cycle. The denominator represents the time and the amount of stationary phase required to produce that mass of protein. Maximization of the production rate will allow the largest quantity of purified product to be produced in the shortest amount of time with the least amount of stationary phase.

In order to calculate the production rate PR_i, the yield Y_i must be calculated. For cases in which a finite separation gap (i.e., baseline resolution) existed between the chromatographic bands, the yield is expected to be 100%. For cases in which sample displacement (i.e., touching chromatographic bands) occurred, the yield was calculated from the formula:

$$Y_i = \frac{\int_{t_1}^{t_2} C_i \, \mathrm{d}t}{C_{i,\mathrm{f}} t_\mathrm{f}} \tag{2}$$

where the cut times t_1 and t_2 are selected to maximize the yield at the specified purity.

Table 1
Optimization variables

Variable	Type	Comments
Production rate, PR_i	Objective function	The ratio of the mass of protein purified to the amount of time and stationary phase required to accomplish the separation.
Feed stream constituents	Parameter	In this study: α-chymotrypsinogen A, cytochrome c, lysozyme, and four hypothetical components
Feed concentrations	Parameter	In this study: 0.2 mM
Stationary phase material	Parameter	In this study: strong cation exchanger
pH	Parameter	In this study: pH 6.0
Eluting salt	Parameter	In this study: sodium chloride
Feed time, τ_f, gradient slope, G_{slope}	Decision variables	Selected in order to maximize the production rate
Maximum protein concentration, C_{max}	Constraint	Implemented at 1.0 mM for comparison with the unconstrained system
Purity, p_i	Constraint	Percentage of the product that is attributable to the desired protein. In this study: p_i >99%.
Yield, Y_i	Constraint	Percentage of the product recovered by the separation process. In this study: Y_i >95%.
Separation gap, τ_{gap}	Constraint	For values of τ_{gap} greater than zero, it is assumed that purity and yield will be 100%.

2.1.2. Parameters

Parameters are variables which cannot be manipulated during the optimization process. For this study of the optimization of preparative linear gradient chromatography, the feed stream constituents were chosen from: α-chymotrypsinogen A, cytochrome c, lysozyme, and four artificial proteins (sets of SMA adsorption parameters) selected to have similar adsorption properties to actual proteins. Although most complex bioseparation problems involve more than three components, one can generally classify the impurities present in the feed stream as those which are more or less strongly retained than the component of interest. Thus, three component systems offer a means to address many of the challenges offered by complex feed mixtures while allowing a precise mathematical treatment to be carried out.

In practice, the concentrations of both the product and the contaminants may vary widely. In the work described below, relatively concentrated feed streams were employed. However, the effect of a substantially more dilute feed stream was considered to put the optimization results in context.

In addition, Table 1 categorizes the stationary phase, pH, and eluting salt as parameters. In practice, the chromatographer examines the performance of many stationary phase/pH/eluting salt combinations in an attempt to maximize the selectivity of the chromatographic system. The focus of this paper will be the process of optimization that goes on after the stationary phase, operating pH, and eluting salt are selected. In this paper, a strong cation exchanger was employed at pH 6.0 with sodium phosphate as the eluting salt.

2.1.3. Decision variables

During optimization, the values of the decision variables are selected to maximize the objective function. In this study the effects of two decision variables, the feed time, τ_f, and the gradient slope, G_{slope}, were considered. Manipulation of these variables allows the mass of protein purified per cycle and the amount of time per cycle to be controlled. Proper selection of the feed volume and gradient slope will allow the largest amount of protein to be purified in the shortest amount of time.

2.1.4. Constraints

In most real processes, the values of the decision variables may not be selected without considering constraints (i.e., pre-specified requirements on the variables of the problem). Four important constraints are: maximum protein concentration, purity, yield,

and separation gap width. Maximum protein concentration is an example of a physical constraint of the process. Care must be taken to insure that the components present in the feed solution do not become excessively concentrated at the risk of aggregation, precipitation, viscous fingering, and other phenomena that can adversely effect the separation. In contrast, purity, yield, and separation gap width are all constraints that are defined by the efficiency of the purification system and by the desired quality of the product. Each of these four constraints will be discussed below.

2.2. Multicomponent equilibrium

The Steric Mass Action (SMA) formalism is a three parameter model of ion exchange designed specifically for representation of multicomponent protein-salt equilibrium in ion-exchange chromatography. In the case of a dilute protein solution, it reduces to the model originally proposed by Boardman and Partridge [16]. However, as the concentration of protein bound to the stationary phase rises, the model takes into account the effect of steric shielding on the binding capacity of the stationary phase. As a result, it is capable of predicting the multicomponent protein adsorption under dilute and concentrated conditions.

The SMA formalism represents this adsorption process as a stoichiometric exchange of mobile phase protein and bound counterions [14]:

$$C_i + \nu_i \bar{Q}_1 \Leftrightarrow Q_i + \nu_i C_1 \quad i = 2,...,NC \tag{3}$$

where C_i and Q_i refer to the concentration of protein in the mobile phase and on the stationary phase, C_1 refers to the concentration of salt in the mobile phase, and $\bar{Q}_1$ refers to the concentration of bound salt available for exchange. The equilibrium constant of the exchange reaction may be written:

$$K_{1i} = \left(\frac{Q_i}{C_i}\right)\left(\frac{C_1}{\bar{Q}_1}\right)^{\nu_i} \quad i = 2,...,NC \tag{4}$$

Each protein molecule may sterically shield some salt counterions on the adsorptive surface. The quantity of salt counterions blocked by a particular protein will be proportional to the concentration of that protein on the surface:

$$\hat{Q}_{1i} = \sigma_i Q_i \quad i = 2,...,NC \tag{5}$$

Electroneutrality requires that:

$$\Lambda = \bar{Q}_1 + \sum_{i=2}^{NC} (\nu_i + \sigma_i) Q_i \tag{6}$$

Eq. (4) and Eq. (6) constitute a system of NC nonlinear equations which describes the multicomponent equilibrium.

2.3. Mass transport equations

The model employed to describe mass transport in this work is a single parameter, lumped dispersion model [29,30]. Eq. (7) describes mass transport in the packed bed of a chromatography column:

$$-\left(\frac{D_i}{u_0 L}\right)\frac{\partial^2 C_i}{\partial x^2} + \frac{\partial C_i}{\partial x} + \frac{\partial C_i}{\partial \tau} + \frac{1-\varepsilon}{\varepsilon}\frac{\partial Q_i}{\partial \tau} = 0 \tag{7}$$

where $x = X/L$ is a nondimensional measure of axial position, $\tau = t/t_0$ is a nondimensional measure of time, D_i is the effective dispersion coefficient, u_0 is the chromatographic velocity, L is the column length, and ϵ is the total porosity of the column. The stationary phase is assumed to be in equilibrium with the mobile phase:

$$Q_i = F_i(C_1, C_2, \ldots C_{NC}) \tag{8}$$

The equilibrium expression F_i is the SMA formalism discussed above. Because the mass transport equations include the assumption of local equilibrium, the use of this type of model is restricted to relatively small stationary phase particles such as those employed in this study. In order to model the impact of mass transport resistance between the mobile and stationary phase, a more extensive mass transport model could be employed [10,13].

In order to define a solution, appropriate initial

and boundary conditions must be supplied. The initial conditions are:

$$C_1(0, x) = C_{1,f} \quad (9a)$$

$$C_i(0, x) = 0 \quad i \neq 1 \quad (9b)$$

$$Q_1(0, x) = \Lambda \quad (9c)$$

$$Q_i(0, x) = 0 \quad i \neq 1 \quad (9d)$$

where $C_{1,f}$ represents the carrier sodium ion concentration at the inlet of the column. During operation the counterion concentration varies with time:

$$C_1(0 < \tau < \tau_f, 0) = C_{1,f} \quad \text{(Loading)} \quad (10a)$$

$$C_1(\tau > \tau_f, 0) = C_{1,f} + [G_{slope} \cdot (\tau - \tau_f)] \text{ (Gradient)} \quad (10b)$$

where τ_f is the length of the feed pulse and G_{slope} is the gradient slope.

The column is loaded with protein during the feed cycle:

$$C_i(0 < \tau < \tau_f, 0) = C_{i,f} \quad \text{(Loading)} \quad (11a)$$

$$C_i(\tau > \tau_f, 0) = 0 \quad \text{(Gradient)} \quad (11b)$$

The study conducted below will employ three proteins (NC=4). The first protein (α-chymotrypsinogen A) will represent the low affinity impurities, the second protein (cytochrome c) will represent the product, and the third protein (lysozyme) will represent the high affinity impurities.

2.4. Solution of model equations

In order to solve this system of partial differential equations, a numerical technique developed by Guiochon and coworkers was employed [29,30]. In this technique, a simple relation exists between the observed efficiency of the chromatography column, the effective dispersion coefficient of Eq. (7), and the dimensions of the finite difference grid:

$$\frac{H}{L} = \frac{2D_i}{Lu_0} = \Delta x - \frac{1}{1 + k'} \Delta \tau \quad (12)$$

where H is the height equivalent to a theoretical plate, L is the column length, k' is the capacity factor in linear chromatography, Δx is the step size in the distance dimension, and $\Delta \tau$ is the step size in the time dimension.

The model described above is employed throughout this manuscript to simulate protein separations by linear gradient chromatography. Simulated chromatograms were generated with a computer program written in FORTRAN. The program was run on an IBM ES/9000 Model 580 mainframe computer using IBM VS FORTRAN under the MTS operating system.

3. Experimental

3.1. Materials

Sodium monobasic phosphate, sodium dibasic phosphate, α-chymotrypsinogen A, cytochrome c, and lysozyme were purchased from Sigma Chemicals (St. Louis, MO, USA). Sodium chloride was purchased from Aldrich Chemical (Milwaukee, WI, USA). o-Phosphoric acid was purchased from Fisher Scientific (Rochester, NY, USA). The strong cation-exchange column employed in this work (54 × 5 mm I.D., 15 μm) was a gift from Pharmacia Biotech AS (Lilistrom, Norway). POROS R/H reversed-phase chromatographic column (100 × 4.6 mm I.D.) was purchased from PerSeptive Biosystems (Cambridge, MA, USA).

3.2. Apparatus

The chromatograph employed in this work consisted of two Model P-500 pumps (Pharmacia, LKB, Uppsala, Sweden) connected to the chromatographic column via a Model MV-7 injector (Pharmacia, LKB). During parameter estimation, the column effluent was monitored using a Model 757 Spectro-

flow UV–VIS absorbance detector (Applied Biosystems, Foster City, CA, USA) and a Powermate 2 personal computer (NEC, Tokyo, Japan) running Maxima 820 data collection software (Waters Chromatography Division, Millipore). During gradient experiments fractions of the column effluent were collected directly from the column using Model 2212 Helirac fraction collector (Pharmacia, LKB). During fraction analysis, a Spectroflow 757 UV–VIS absorbance detector (Applied Biosystems) was employed to monitor the column effluent, and a model C-R3A Chromatopac integrator (Shimadzu, Kyoto, Japan) was employed for data acquisition and analysis.

3.3. Procedures

3.3.1. Parameter estimation

The estimation of the SMA equilibrium parameters which appear in Table 2 has been discussed previously [15,23]. In order to estimate the characteristic charges ν_i and equilibrium constants K_{1i} of the proteins, linear elution experiments were conducted at various mobile phase salt concentrations. The resulting data was fitted to the following linearized equation:

$$\log (k_i') = \log (\beta k_{1i} \Lambda^{\nu_i}) - \nu_i \log (C_1) \quad (13)$$

This fitting procedure provided estimates of the characteristic charges ν_i and equilibrium constants K_{1i} of the proteins. In order to estimate the steric factors σ_i, nonlinear frontal experiments were carried out over a range of mobile phase salt concentrations.

$$C_{2,\mathrm{SMA}} = \left(\frac{C_{1,\mathrm{f}}}{\Lambda - (\nu_i + \sigma_i) Q_{2,\mathrm{f}}} \right)^{\nu_i} \frac{Q_{2,\mathrm{f}}}{K_{1i}} \quad (14)$$

Eq. (14) was used in conjunction with the experimental protein isotherms in order to estimate the steric factors σ_i. The residuals between the experimental protein concentration ($C_{2,\mathrm{f}}$) and the estimate of the protein concentration ($C_{2,\mathrm{SMA}}$) obtained from Eq. (14) may be calculated as a function of the steric factor. Minimization of the sum of squares of the residuals using a Newton–Raphson technique established the estimated steric factor.

The linear gradient experiments were carried out at 0.5 ml/min. In order to estimate the appropriate plate height to be employed in Eq. (12), the ef-

Table 2
Parameters employed in simulations

Solute	Characteristic charge (ν_i)	Steric factor (σ_i)	Equilibrium constant (K_{1i})
Counter ion			
Sodium ion	1.00	0.00	1.00
Low affinity impurities			
α-Chymotrypsinogen A	5.03	7.43	$1.35 \cdot 10^{-2}$
α-Chymotrypsinogen A′	6.29	7.43	$3.60 \cdot 10^{-3}$
α-Chymotrypsinogen A″	5.03	3.72	$1.35 \cdot 10^{-2}$
Products			
Cytochrome *c*	5.67	27.4	$4.50 \cdot 10^{-2}$
Cytochrome *c*′	5.67	13.7	$4.50 \cdot 10^{-2}$
High affinity impurities			
Lysozyme	6.14	0.00	$2.12 \cdot 10^{-1}$
Lysozyme′	6.14	0.00	$7.07 \cdot 10^{-2}$

Column: 54 mm × 5 mm I.D.
Column capacity (Λ): 525 m*M*.
Void fraction (ε): 0.73.
Flow-rate: 0.5 ml/min.
Plates/meter at $k'=2$ (N): 5556 m^{-1}.

ficiency of the column at that velocity was determined by measuring the width at half-height of separate dilute injections of α-chymotrypsinogen A, cytochrome *c*, and lysozyme. An average of the resulting efficiencies, 5556 was employed.

3.3.2. Linear gradient chromatography

For the linear gradient experiments, Buffer A consisted of a 30 m*M* sodium phosphate solution pH 6.0. Buffer B contained 470 m*M* sodium chloride in 30 m*M* sodium phosphate buffer, pH 6.0. Following equilibration of the column with Buffer A, the feed solution was introduced into the column. After an appropriate feed volume was loaded, the linear gradient was initiated. The gradient program was timed so that the mobile phase salt concentration at the column inlet would begin to rise immediately after the injection, as described by the boundary conditions (10b). Fractions of the column effluent were collected and analyzed for protein concentration using the procedure described below. The experimental conditions are presented in the figure captions.

3.3.3. Protein analysis

Analysis of the fractions collected during linear gradient operation was performed by gradient RPLC. The fractions were diluted 5- to 100-fold. Buffer A contained 50 m*M* sodium phosphate pH 2.2. Buffer B contained 50 m*M* sodium phosphate pH 2.2 and 70% acetonitrile. The gradient program started at 25% B and ended at 90% B in 7 min at a flow-rate of 0.8 ml/min. The proteins were detected using a UV–Vis detector set to 280 nm. The compositional data from the protein analysis was used to generate a histogram representing each step gradient experiment.

4. Results and discussion

4.1. Model verification

Three linear gradient experiments were carried out with protein loadings and gradient slopes typical of the conditions employed during the optimization study described below. The results of these experiments were compared to simulated chromatograms in order to verify the model's accuracy.

For the first separation, a solution of 0.2 m*M* α-chymotrypsinogen A, 0.2 m*M* cytochrome *c*, and 0.2 m*M* lysozyme in Buffer A was injected into the column. After loading 2.0 column dead volumes of the feed solution, a linear gradient with a slope of 25 m*M* sodium ion concentration per column dead volume was introduced into the column. Fig. 1 shows a comparison between this experiment and the simulated chromatogram produced by the model. In the experimental chromatogram (Fig. 1a), three peaks are visible representing the three feed stream components α-chymotrypsinogen A, cytochrome *c*,

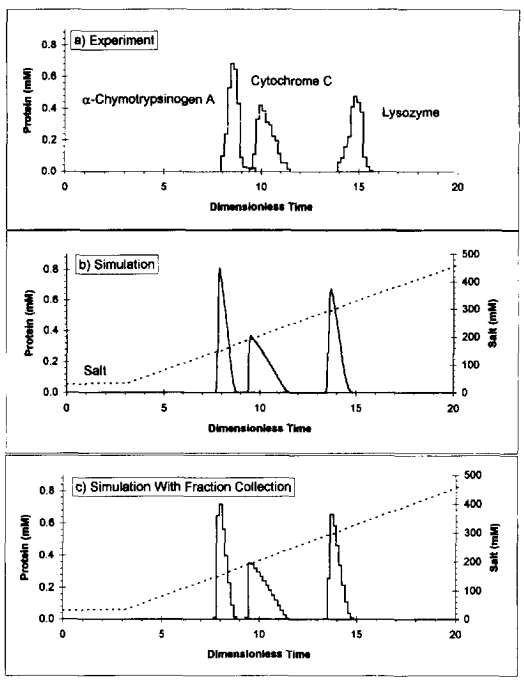

Fig. 1. Comparison of simulated and experimental chromatograms: (a) Reconstructed experimental linear gradient chromatogram. Feed injection: 2.0 column dead volumes of 0.2 m*M* α-chymotrypsinogen A, 0.2 m*M* cytochrome *c*, and 0.2 m*M* lysozyme in 30 m*M* sodium phosphate. Gradient slope: 25 m*M* sodium ion per column dead volume. Operating conditions: 0.5 ml/min, pH 6.0, 125 μl fractions. (b) Simulated chromatogram without fraction collection. (c) Simulated chromatogram with fraction collection.

and lysozyme. Fig. 1b depicts the result of a chromatographic simulation of this experiment. A comparison of Fig. 1a and Fig. 1b reveals good agreement between the experimental and simulated retention times, concentrations, and peak shapes. In particular, the asymmetric peak shape characteristic of nonlinear chromatography is visible in both the experiment and simulation. In Fig. 1c, fraction collection was simulated by pooling the simulated column effluent into 0.16 column dead volume fractions. The resulting profiles are discontinuous and closely resemble those in the experimental chromatogram (Fig. 1a) which was generated by analysis of the collected fractions.

A second experiment was performed in which 6.0 column dead volumes of a solution of 0.2 m*M* α-chymotrypsinogen A, 0.2 m*M* cytochrome *c*, and 0.2 m*M* lysozyme in Buffer A was injected into the column. Again, a gradient slope of 25 m*M* sodium ion concentration per column dead volume was employed. In the experimental chromatogram (Fig. 2a), three peaks are again visible representing the three feed components. Fig. 2b depicts the result of a chromatographic simulation of this experiment. A comparison of Fig. 2a and Fig. 2b reveals good agreement between the experimental and simulated concentration profiles, including the sample displacement of α-chymotrypsinogen A by cytochrome *c*. This type of induced sample displacement has been observed previously in reversed-phase chromatography [31]. Fig. 2c presents the simulated chromatogram with fraction collection in order for the effect of pooling fractions to be assessed.

A third experiment was performed in which 8.0 column dead volumes of the same feed solution was injected into the column. A shallower gradient slope of 10 m*M* sodium ion concentration per column dead volume was employed in order to avoid excessive concentration of the protein bands at this high column loading. In the experimental chromatogram (Fig. 3a), the three peaks of α-chymotrypsinogen A, cytochrome *c*, and lysozyme have become quite broad, exhibiting substantial nonlinear effects. Fig. 3b depicts the result of a chromatographic simulation of this experiment. A comparison of Fig. 3a and Fig. 3b reveals that the model is indeed capable of predicting the nonlinear adsorption behavior as well

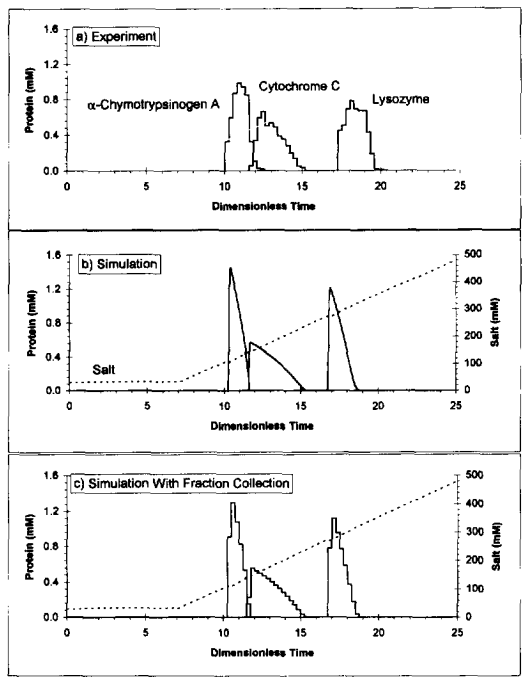

Fig. 2. Comparison of simulated and experimental chromatograms: (a) Reconstructed experimental linear gradient chromatogram. Feed injection: 6.0 column dead volumes of 0.2 m*M* α-chymotrypsinogen A, 0.2 m*M* cytochrome *c*, and 0.2 m*M* lysozyme in 30 m*M* sodium phosphate. Gradient slope: 25 m*M* sodium ion per column dead volume. Operating conditions: 0.5 ml/min, pH 6.0, 200 μl fractions. (b) Simulated chromatogram without fraction collection. (c) Simulated chromatogram with fraction collection.

as the sample displacement of α-chymotrypsinogen by cytochrome *c*. Fig. 3c presents the simulated chromatogram with fraction collection in order for the effect of pooling fractions to be assessed.

Together, Fig. 1, Fig. 2, and Fig. 3 clearly demonstrate the ability of the chromatographic model to represent linear gradient chromatography under conditions of multicomponent competitive binding. Some errors in the model's predictions can be seen in these comparisons of experiment and simulation. Possible causes of these errors include (1) the relatively simple mass transport model employed, (2) the kinetics of adsorption and desorption and, (3) heterogeneity of the proteins employed.

Since the model is able to correctly predict the

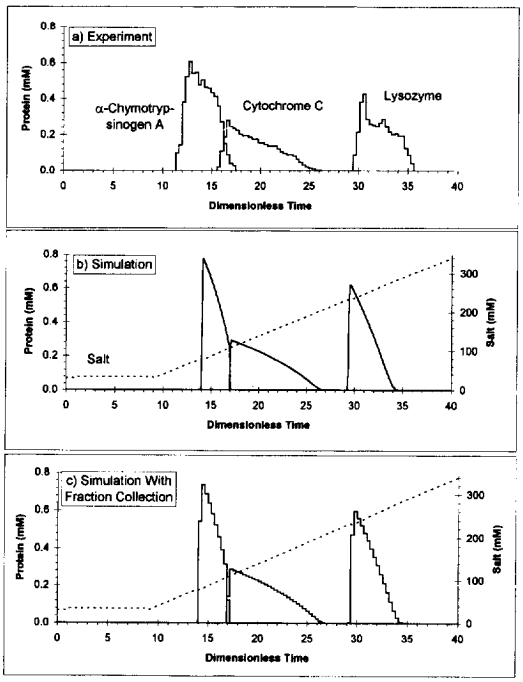

Fig. 3. Comparison of simulated and experimental chromatograms: (a) Reconstructed experimental linear gradient chromatogram. Feed injection: 8.0 column dead volumes of 0.2 m*M* α-chymotrypsinogen A, 0.2 m*M* cytochrome *c*, and 0.2 m*M* lysozyme in 30 m*M* sodium phosphate. Gradient slope: 10 m*M* sodium ion per column dead volume. Operating conditions: 0.5 ml/min, pH 6.0, 250 μl fractions. (b) Simulated chromatogram without fraction collection. (c) Simulated chromatogram with fraction collection.

course of development of preparative gradient separations, it can be employed with confidence to rapidly and efficiently explore the behavior of this protein separation system. Furthermore, the optimization behavior of this system can now be considered in detail with good confidence in the conclusions of the study.

4.2. Linear Gradient Chromatography

This study of the optimization of linear gradient chromatography will begin by considering the effect of the decision variables (τ_f and G_{slope}) and the constraints (maximum protein concentration, separation gap width, purity, and yield) on the separation of cytochrome *c* from α-chymotrypsinogen and lysozyme. Subsequently, the effect of changes in the adsorption properties of the feed components will be considered.

4.2.1. Protein adsorption behavior of α-chymotrypsinogen A, cytochrome c, and lysozyme

The first feed stream which will be considered contains the proteins α-chymotrypsinogen A (representing a low affinity impurity), cytochrome *c* (representing the product), and lysozyme (representing a high affinity impurity). Fig. 4 presents a log (k') versus log(salt concentration) plot of the proteins α-chymotrypsinogen A, cytochrome *c*, and lysozyme. Under isocratic conditions, the linear retention behavior may be predicted by a simple examination of the log (k') versus log (salt concentration) plot. When a linear gradient is employed, the loading salt concentration C_0 and the gradient slope G_{slope} play an important role in determining the observed elution time. If a relatively small mass of protein is loaded, then the elution time may be calculated using Snyder's linear solvent strength theory (Appendix). For greater protein loads, nonlinear adsorption becomes important, and the chromatographic peaks emerge from the column earlier than predicted by Snyder's theory.

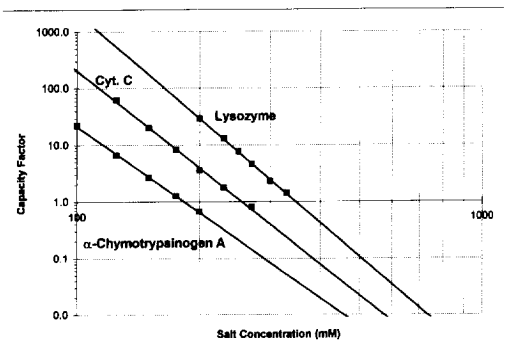

Fig. 4. Log (k') versus log(salt concentration) plot for α-chymotrypsinogen A, cytochrome *c*, and lysozyme. Symbols (■) represent data taken under infinite dilution conditions; lines are SMA representation of data.

4.2.2. Feed volume

As the feed volume is increased, nonlinear adsorption will begin to affect the chromatographic behavior of the feed stream constituents even when the feed stream is dilute. This is to be expected since during loading under low salt conditions the feed components will have a high affinity for the stationary phase and will thus be concentrated during the loading step.

Fig. 5a depicts a simulated chromatogram resulting from the injection of 2.0 column dead volumes of 0.2 m*M* α-chymotrypsinogen A, 0.2 m*M* cytochrome *c*, and 0.2 m*M* lysozyme in 30 m*M* sodium phosphate followed by a gradient of 10 m*M* sodium ion concentration per column dead volume. It is possible to estimate the infinite dilution elution time of the three peaks in this Figure using the linear solvent strength theory (LSS) (Appendix). LSS predicts infinite dilution elution times of 14.7, 20.2, and 26.9 column volumes for α-chymotrypsinogen A, cytochrome *c*, and lysozyme, respectively. Examination of Fig. 5a reveals that all three peaks break through substantially before the expected elution time based on LSS.

If the feed volume is increased to 6.0 column dead volumes, the model predicts that the chromatogram will resemble Fig. 5b. As seen in the figure, under these conditions, α-chymotrypsinogen A undergoes sample displacement by cytochrome *c*. Because of this sample displacement, the infinite dilution time of α-chymotrypsinogen A predicted by LSS (18.7 column dead volumes) is quite different from the observed end of that peak at 16.5.

4.2.3. Gradient slope

In Fig. 5a, it was observed that the separation gap between the first two peaks α-chymotrypsinogen A and cytochrome *c* was relatively wide when a gradient of 10 m*M* sodium ion concentration per column volume was employed. As seen in Fig. 5c, an increase of the gradient slope to 50 m*M* sodium ion concentration per column volume leads to substantially narrower and more concentrated chromatographic bands with narrower gaps between the bands.

In Fig. 5d, both the gradient slope and the feed volume are increased at the same time. The elution concentrations of α-chymotrypsinogen A and lysozyme are increased by an order of magnitude over their feed concentrations. Such high protein concentrations could lead to aggregation, precipitation, or viscous fingering within the chromatographic column. Clearly, protein concentration should be

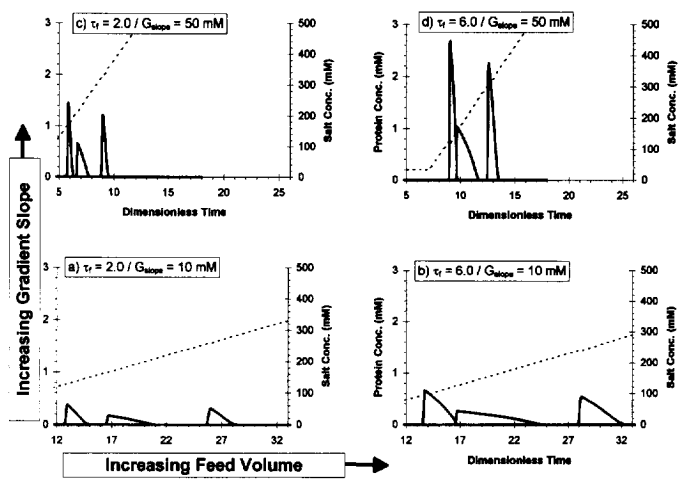

Fig. 5. Effect of feed volume and gradient slope. Simulation conditions: feed: 0.2 m*M* α-chymotrypsinogen A, 0.2 m*M* cytochrome *c*, and 0.2 m*M* lysozyme in 30 m*M* sodium phosphate; operating conditions: 0.5 ml/min, pH 6.0; τ_f and G_{slope}: as indicated on figures.

carefully monitored during design of any gradient separation.

4.3. Optimum production rate curves

In order to establish the optimum gradient slope for a given feed volume, a FORTRAN subroutine was written based on the iterative optimization scheme depicted in Fig. 6. Prior to computer optimization of the problem, appropriate values of the parameters and constraints were specified (steps 1 and 2 in Fig. 6). An initial feed volume and gradient slope were then specified (step 3 in Fig. 6). Subsequently, the subroutine was employed to calculate the optimum gradient slope and feed volume for the given separation problem.

To locate the optimum gradient slope in separation problems where selectivity reversal did not occur, the iterative loop (step 4 in Fig. 6) utilized the following rules to maximize the production rate for a given feed volume subject to the constraints: (1) The production rate increases with increasing gradient slope when constraints on yield and purity are met. (2) The maximum protein concentration of each chromatographic band increases with increasing gradient slope. (3) The gap width between two adjacent bands decreases with increasing gradient slope. (4) The yield remains constant or decreases with increasing gradient slope. For a given feed volume and set of constraints, the program calculated the optimum gradient slope within ± 0.5 mM sodium ion concentration per column volume.

The first problem which was examined was the separation of cytochrome c (product) from a mixture containing α-chymotrypsinogen A (the low affinity impurity) and lysozyme (the high affinity impurity) with a separation gap constraint of 0.5 column dead volumes and no constraint on maximum protein concentration. Table 3 presents data from that optimization. Each time an iteration within step 4 in Fig. 6 is completed, the result is an optimum gradient slope for that particular feed volume. In Table 3 separation problems # 1 through # 9, the optimum gradient slope, yield, purity, and production rate for a series of feed volumes ranging from 0.5 to 4.5 column dead volumes are presented. Examination of separation problems #1 through #9 reveals that the optimum gradient slope decreases with increasing feed volume, as expected. Because a finite separation gap was maintained for each of these feed volumes, the purity and yield are both 100%. Of particular interest is the production rate. In order to calculated the production rate of cytochrome c ($PR_{\text{cytochrome } c}$), the cycle time must be calculated. In this work, the cycle time was represented by the expression:

$$t_{cyc} = t_0(\tau_f + \tau_{sep} + 7.0) \quad (15)$$

where τ_f is the time required to load the feed, τ_{sep} is the time from the end of the feed injection to the time that the product finishes eluting from the column, and t_0 is the transit time of an unretained component through the column. The cycle time represents an estimate of the time required to load the column (τ_f), to perform the separation (τ_{sep}), and to regenerate and re-equilibrate the column with the initial salt concentration (7.0 t_0). The production rate data in Tables 3, 4 and 5 was calculated using this definition of cycle time.

In Fig. 7, the production rate data for the initial separation problem (#1 through #9 of Table 3) is depicted by open circles (○). Each point represents a separation achieved using the optimum gradient slope for that particular feed volume. As can be seen from this plot, the production rate initially increases linearly with feed volume. As the feed volume becomes larger, the steady decrease of the optimum gradient slope results in longer separation times. This increase in the separation time causes the production rate to plateau and begin to decline. The maximum production rate of 2.25 μmol/(ml h) is obtained at a

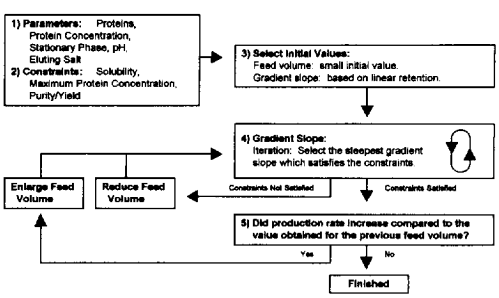

Fig. 6. Iterative optimization scheme for linear gradient chromatography.

Table 3
Optimum separation conditions for baseline resolution

Separation problem			Constraints		Optimum slope and productivity				
Ident.	Feed stream[a]	τ_f	C_{max} (mM)	τ_{gap}	G_{slope} (mM)	Yield (%)	Purity (%)	$PR_{cytochrome\ c}$ (μmol/ml h)	PR (mg/ml h)
# 1	a	0.5	None	0.5	51	100	100	0.78	9.7
# 2	a	1.0	None	0.5	37	100	100	1.36	16.8
# 3	a	1.5	None	0.5	31	100	100	1.87	23.2
# 4	a	2.0	None	0.5	23	100	100	2.15	26.6
# 5	a	2.5	None	0.5	16	100	100	2.25	27.9
# 6	a	3.0	None	0.5	10	100	100	2.18	27.0
# 7	a	3.5	None	0.5	7	100	100	1.97	24.4
# 8	a	4.0	None	0.5	4	100	100	1.58	19.6
# 9	a	4.5	None	0.5	2	100	100	1.18	14.6
# 10	a	0.5	1.0	0.5	51	100	100	0.78	9.7
# 11	a	1.0	1.0	0.5	37	100	100	1.36	16.8
# 12	a	1.5	1.0	0.5	31	100	100	1.87	23.2
# 13	a	2.0	1.0	0.5	23	100	100	2.15	26.6
# 14	a	2.5	1.0	0.5	16	100	100	2.25	27.9
# 15	a	3.0	1.0	0.5	10	100	100	2.18	27.0
# 16	a	3.5	1.0	0.5	7	100	100	1.97	24.4
# 17	a	4.0	1.0	0.5	4	100	100	1.58	19.6
# 18	a	4.5	1.0	0.5	2	100	100	1.18	14.6

a = 0.2 mM of α-chymotrypsinogen A, cytochrome c, and lysozyme.

feed volume of 2.5 column dead volumes (separation problem #5 in Table 3). The simulated chromatogram which corresponds to this separation is shown in Fig. 8a.

4.3.1. *Effect of feed stream concentration*

Proteins exhibit high affinity for the stationary phase under low salt conditions leading to extremely nonlinear (square) isotherms. Due to this strong binding, similar masses of protein may be loaded onto the same length of column under dilute and concentrated conditions [28]. As a result, for both dilute and concentrated feed streams, the time required to accomplish the separation after the feed has been loaded will be similar. The major difference in

Table 4
Optimum separation conditions for sample displacement

Separation problem			Constraints		Optimum slope and productivity				
Ident.	Feed stream[a]	τ_f	C_{max} (mM)	τ_{gap}	G_{slope} (mM)	Yield (%)	Purity (%)	$PR_{cytochrome\ c}$ (μmol/ml h)	PR (mg/ml h)
# 19	a	2.0	None	0.0	300	100	99	3.74	46.3
# 20	a	4.0	None	0.0	300	100	99	6.33	78.3
# 21	a	8.0	None	0.0	297	96	99	9.33	115.4
# 22	a	1.0	1.0	0.0	48	100	99	1.48	18.3
# 23	a	2.0	1.0	0.0	31	100	99	2.43	30.0
# 24	a	4.0	1.0	0.0	21	100	99	3.78	46.8
# 25	a	6.0	1.0	0.0	16	100	99	4.77	59.1
# 26	a	8.0	1.0	0.0	13	100	99	5.50	68.1
# 27	a	10.0	1.0	0.0	11	100	99	6.05	74.9
# 28	a	12.0	1.0	0.0	10	100	99	6.63	82.1
# 29	a	14.0	1.0	0.0	6	100	99	5.94	73.5

a = 0.2 mM of α-chymotrypsinogen A, cytochrome c, and lysozyme.

Table 5
Optimum separation conditions for artificial feed streams

Separation problem			Constraints		Optimum slope and productivity				
Ident.	Feed stream[a]	τ_f	C_{max} (mM)	τ_{gap}	G_{slope} (mM)	Yield (%)	Purity (%)	$PR_{cytochrome\ c}$ (μmol/ml h)	PR (mg/ml h)
# 30	b	2.5	None	0.5	5	100	100	1.18	14.6
# 31	b	2.5	1.0	0.5	5	100	100	1.18	14.6
# 32	b	6.0	1.0	0.0	17	100	99	4.84	59.9
# 33	c	2.5	None	0.5	10	100	100	1.81	22.5
# 34	c	2.5	1.0	0.5	10	100	100	1.81	22.5
# 35	c	6.0	1.0	0.0	16	100	99	4.78	59.1
# 36	d	2.5	None	0.5	16	100	100	2.24	27.7
# 37	d	2.5	1.0	0.5	16	100	100	2.24	27.7
# 38	d	6.0	1.0	0.0	12	100	99	4.27	52.8
# 39	e	2.5	None	0.5	32	100	100	2.97	36.7
# 41	e	2.5	1.0	0.5	28	100	100	2.82	34.9
# 42	e	6.0	1.0	0.0	17	100	99	4.83	59.8

b = 0.2 mM of α-chymotrypsinogen A′, cytochrome c, and lysozyme; c = 0.2 mM of α-chymotrypsinogen A, cytochrome c, and lysozyme′; d = 0.2 mM of α-chymotrypsinogen A″, cytochrome c, and lysozyme; e = 0.2 mM of α-chymotrypsinogen A, cytochrome c′, and lysozyme.

processing time for dilute and concentrated feed streams will be the time required to load the feed.

In order to see the effect on the production rate curve, the production rate of a feed stream of 0.0002 mM α-chymotrypsinogen A, 0.0002 mM cytochrome c, and 0.0002 mM lysozyme in 30 mM sodium phosphate was approximated in the following manner. The loading time was calculated as:

$$\tau_{f,\ low\ conc.} = (1000 \cdot \tau_{f,\ high\ conc.}) \quad (16)$$

Assuming identical separation time (t_{sep}) and regeneration/re-equilibration time (7.0 * t_0), the chromatographic cycle time for this extremely dilute feed stream is given by:

$$t_{cyc,\ low\ conc.} = t_0(\tau_{f,\ low\ conc.} + \tau_{sep} + 7.0) \quad (17)$$

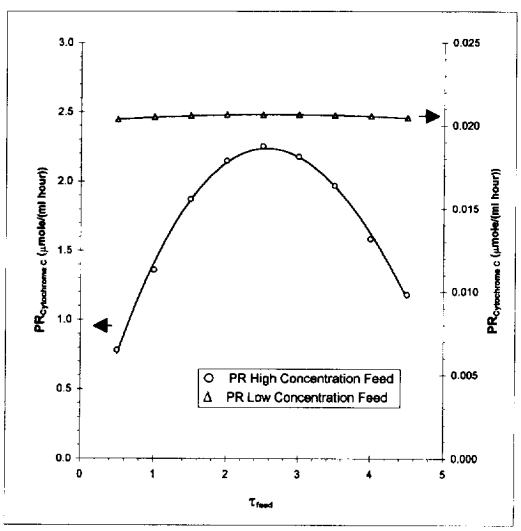

Fig. 7. Optimum cytochrome c production rate curves for α-chymotrypsinogen A, cytochrome c, and lysozyme feed stream with 0.5 separation gap constraint. ○=high concentration feed ($t_{cyc}=t_0$ ($\tau_f+\tau_{sep}+7.0$)). △ = low concentration feed ($t_{cyc}=t_0$ ($\tau_{f,low\ conc.}+\tau_{sep}+7.0$)).

In Fig. 7, the production rate data for the dilute feed stream is depicted by open triangles (Δ). Since the cycle time becomes essentially equal to the loading time when a very dilute feed stream is loaded, the production rate is insensitive to the feed volume. As a result, similar amounts of protein may be produced on an hourly basis using large or small injections.

4.3.2. Maximum protein concentration constraint

Preparative linear gradient chromatography can substantially concentrate proteins. However, excessive concentration can lead to many phenomena that can have a negative impact on the separation such as aggregation, precipitation, or viscous fingering. As seen above, a reduction in gradient slope (with feed

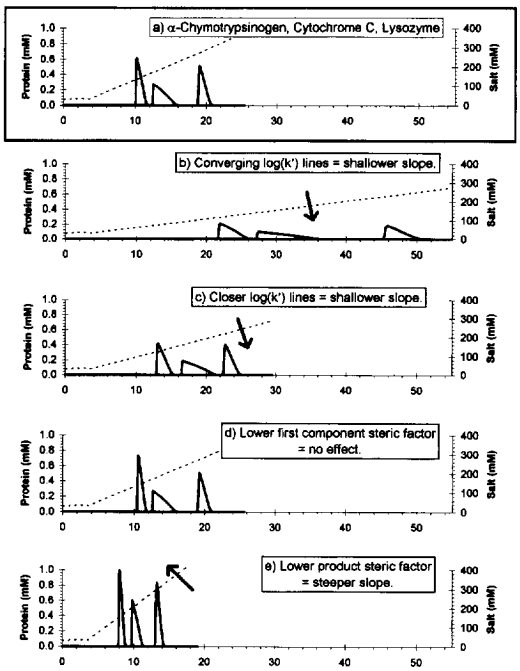

Fig. 8. Optimum separations with 0.5 gap width and 1.0 m*M* maximum protein concentration constraints. Simulation conditions: feed: 2.5 column dead volumes of 0.2 m*M* each component in 30 m*M* sodium phosphate; operating conditions: 0.5 ml/min, pH 6.0. (a) α-chymotrypsinogen A, cytochrome *c*, and lysozyme (# 14 in Table 3). (b) α-chymotrypsinogen A′, cytochrome *c*, and lysozyme (# 31 in Table 5). (c) α-chymotrypsinogen A, cytochrome *c*, and lysozyme′ (# 34 in Table 5). (d) α-chymotrypsinogen A″, cytochrome *C*, and lysozyme (# 37 in Table 5). (e) α-chymotrypsinogen A, cytochrome *C′*, and lysozyme (# 40 in Table 5).

volume held constant) results in a reduction of the maximum concentration of the chromatographic peaks. Thus, a maximum protein concentration constraint will impose an upper limit on the gradient slope, and this maximum allowable slope will be a function of the feed volume loaded (as well as the properties of the feed stream and the other parameters of the separation).

The optimization problem discussed above (separation problems #1–9 in Table 3; open circles (○) in Fig. 7 and Fig. 9) did not include a maximum protein concentration constraint. Nevertheless, the 0.5 gap width constraint played a significant role in limiting the value of the optimum gradient slope. Examination of Fig. 8a, the optimum separation for

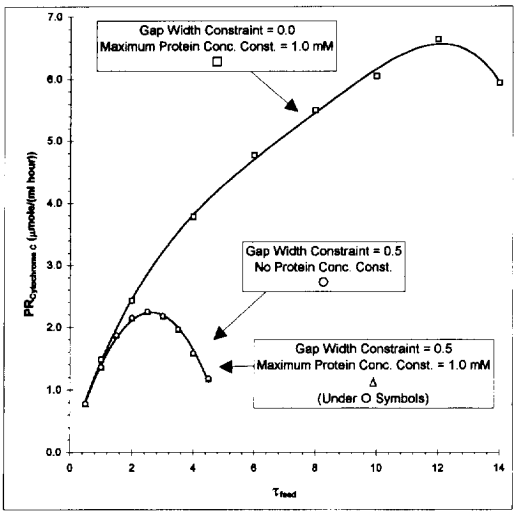

Fig. 9. Optimum cytochrome *c* production rate curves for α-chymotrypsinogen A, cytochrome *c*, and lysozyme feed stream.

this problem, reveals that all of the protein concentrations are below the 1.0 m*M* maximum protein concentration constraint. Thus, for this problem, the 0.5 gap width constraint is more restrictive than the 1.0 m*M* maximum protein concentration constraint. As a result, the optimum curve for the separation problem without a maximum protein concentration constraint in Fig. 9 (○) falls on top of the curve with a 1.0 m*M* constraint on maximum protein concentration (Δ). (This can be verified by comparing the optimized separations # 10 through # 18 in Table 3 with #1 through #9.)

As the separation gap constraint is removed from the separation problem, it becomes possible for sample displacement effects to be observed in the final chromatogram (Fig. 2 and Fig. 3). For separations in which sample displacement is allowed, the maximum protein concentration constraint plays a tremendously important role. Consider the separation of 0.2 m*M* each of α-chymotrypsinogen A, cytochrome *c*, and lysozyme in Buffer A. When sample displacement was allowed and no maximum protein concentration constraint was imposed, the FORTRAN optimization subroutine selected physically impractical steep gradients (separation problems #19 through #21 in Table 4). For two of these feed volumes, the subroutine selected the maximum allowed gradient slope (300 m*M* per column dead

volume, an arbitrary upper limit selected prior to an optimization run). Clearly, in order to avoid such unrealistically steep gradients in sample displacement, it is necessary to include a constraint on the maximum protein concentration.

When a maximum protein concentration constraint of 1.0 m*M* was incorporated into the problem, it was possible to calculate a physically realistic optimum gradient slope. The optimum gradient slopes for fixed values of τ_f are given in Table 4 as separation problems #22 through #29. Examining the Table, the optimum gradient slope can be seen to decrease from 48 to 6 m*M* per column dead volume as the amount of protein increases. Allowing sample displacement also resulted in a significant improvement of the chromatographic productivity described in the next section.

4.3.3. Yield and separation gap width constraints

During this optimization study, when a separation gap constraint was imposed, 100% purity and yield were achieved in all simulated separations. This result was checked experimentally by the linear gradient separation shown in Fig. 1. Although the experimental separation displayed a somewhat smaller degree of separation between the first two components, the experiment still yielded 99% of the cytochrome *c* at 99% purity. This yield could readily be increased to 100% by a slight decrease in the gradient slope.

When sample displacement was allowed, 100% purity and yield were no longer achieved. In Fig. 2 and Fig. 3, the simulated yields were 100% (reduced with simulated fraction collection to 92% and 97%, respectively) while the experiments achieved yields of 92% and 79%, respectively. The high yields achieved in the simulations are likely due to the relatively simple mass transport model that was employed for these simulations [29,30].

In spite of the somewhat lower yields achieved without a constraint on separation gap, sample displacement offers a means to substantially increase the chromatographic productivity of preparative separations. In Fig. 9, it can be seen that the production rates for the base-line resolved (○) and the sample displacement (□) separations are identical at small feed volumes. However, the production rate for separations which include displacement continues to increase long after the other curve has reached its maximum. Thus, a separation which includes displacement will be able to separate significantly more protein in a given amount of time, provided that the yield and purity constraints can be satisfied.

4.4. Consideration of the SMA adsorption parameters

Having discussed the ways that nonlinear adsorption can affect preparative linear gradient separations using the α-chymotrypsinogen A, cytochrome *c*, lysozyme model separation, other potential classes of separations will now be explored by systematically varying the SMA adsorption parameters. Again, three components (a low affinity impurity, a product, and a high affinity impurity) will be employed in these problems. The feed injections will consist of either 2.5 or 6.0 column dead volumes of a solution containing 0.2 m*M* of each of the three components in 30 m*M* sodium phosphate, pH 6.0. A maximum protein concentration constraint of 1.0 m*M* will be employed throughout this section. For some separations, a 0.5 column dead volume gap width constraint will also be included.

4.4.1. Linear adsorption parameters (K_{1i} and ν_i)

The linear adsorption behavior as represented in the SMA formalism by K_{1i} and ν_i is of great importance. Under infinite dilution conditions, these parameters dictate the elution time of the proteins [Appendix A]. In order to assess the importance of these parameters in nonlinear preparative chromatography, two artificial sets of SMA adsorption parameters were generated: α-chymotrypsinogen A′ and lysozyme′. The values of these parameter sets are listed in Table 2, and the log (k') versus log (salt concentration) plots of these hypothetical feed components are shown in Fig. 10.

As seen in Fig. 10, the log (k') versus log (salt concentration) lines of α-chymotrypsinogen A and cytochrome *c* diverge as salt concentration decreases. This indicates an increase in the separation factor of this pair of proteins with decreasing salt concentration. In contrast, the log (k') versus log (salt concentration) lines of α-chymotrypsinogen A′ and cytochrome *c* converge as salt concentration de-

creases (indicating a decrease in the separation factor). This decrease in separation factor can significantly affect the optimum separation conditions. Fig. 8a shows the optimized separation of α-chymotrypsinogen A, cytochrome c, and lysozyme for a feed injection of 2.5 column dead volumes with a maximum protein concentration constraint of 1.0 mM and a separation gap constraint of 0.5. This separation may be compared to the optimized separation of 2.5 column dead volumes of α-chymotrypsinogen A′, cytochrome c, and lysozyme shown in Fig. 8b. As can be seen by comparing these two figures, a shallower gradient is required to separate the α-chymotrypsinogen A′/cytochrome c pair. Thus, the convergence or divergence of the lines in the log (k') versus salt concentration plot plays an important role during the optimization process for a separation gap constrained problem.

If the separation gap constraint is removed, sample displacement can occur. Fig. 11a shows the optimized separation of α-chymotrypsinogen A, cytochrome c, and lysozyme for a feed injection of 6.0 column dead volumes with a maximum protein concentration constraint of 1.0 mM and no separation gap constraint. Comparison of this figure to Fig. 11b, the analogous separation of α-chymotrypsinogen A′, cytochrome c, and lysozyme, reveals that the change in the feed stream has no effect on the optimum gradient slope under these conditions. Since the product is able to effectively displace the first component in both separations, no change in gradient slope was required.

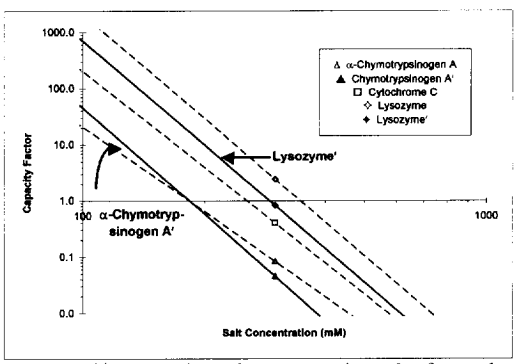

Fig. 10. Log (k') versus log(salt concentration) plot for α-chymotrypsinogen A, α-chymotrypsinogen A′, cytochrome c, lysozyme, and lysozyme′.

The separation of the product cytochrome c from the strongly retained impurity lysozyme can be readily carried out. A decrease of the equilibrium constant of the third component from 0.212 (lysozyme) to 0.0707 (lysozyme′) substantially decreases the separation factor of the second and third components and makes the separation more difficult. This decrease in separation factor can be observed in Fig. 10 by virtue of the fact that the log (k') versus log (salt concentration) line of lysozyme ′ is dramatically closer to the line of the product than the line of lysozyme is. As a result, a shallower gradient slope is required in order to satisfy the separation gap constraint. While the cytochrome c/lysozyme pair may be separated with a 16 mM per column volume

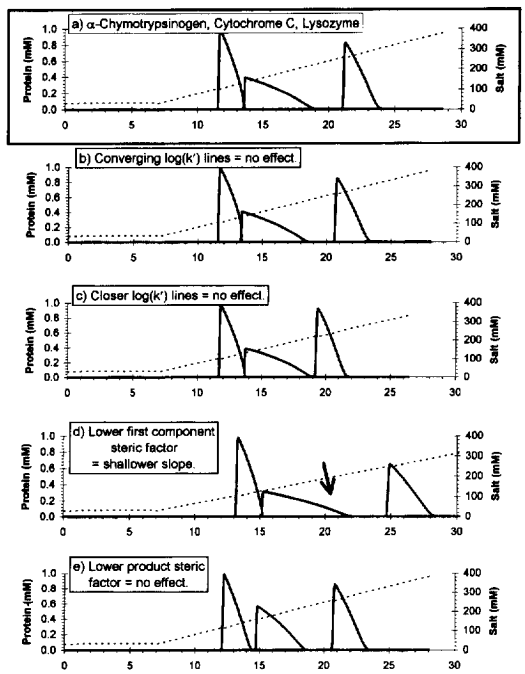

Fig. 11. Optimum separations with 1.0 mM maximum protein concentration constraint and no gap width constraint. Simulation conditions: feed: 6.0 column dead volumes of 0.2 mM each component in 30 mM sodium phosphate; operating conditions: 0.5 ml/min, pH 6.0. (a) α-chymotrypsinogen A, cytochrome c, and lysozyme (# 25 in Table 3). (b) α-chymotrypsinogen A′, cytochrome c, and lysozyme (# 32 in Table 5). (c) α-chymotrypsinogen A, cytochrome c, and lysozyme′ (# 35 in Table 5). (d) α-chymotrypsinogen A″, cytochrome c, and lysozyme (# 38 in Table 5). (e) α-chymotrypsinogen A, cytochrome C', and lysozyme (# 41 in Table 5).

gradient (Fig. 8a), the cytochrome *c*/lysozyme′ pair requires a 10 m*M* gradient (Fig. 8c). Thus, the optimum gradient slope in a three component separation may be determined by the difficulty of separating the product from the low affinity impurity or the high affinity impurity.

The separation of α-chymotrypsinogen A, cytochrome *c*, and lysozyme′ for the case in which the separation gap constraint has been removed is shown in Fig. 11c. Because the last component has not moved sufficiently forward in the final chromatogram to contaminate the product peak, no effect is observed on the optimum gradient slope. However, for extremely low separation factors, it is expected that there would be loss of either yield or purity.

4.4.2. Nonlinear adsorption parameter (σ_i)

In order to examine the effects of nonlinearity on preparative linear gradient separations, two artificial sets of SMA adsorption parameters were generated: α-chymotrypsinogen A″ and cytochrome *c*′. The values of these parameter sets are listed in Table 2.

The parameters of α-chymotrypsinogen A″ are quite similar to α-chymotrypsinogen A, the protein that it replaced in the feed stream; however, the steric factor of α-chymotrypsinogen A″ is half that of α-chymotrypsinogen A. (A decrease in the steric factor results in a higher stationary phase concentration under nonlinear conditions.) Examination of the optimized separation of α-chymotrypsinogen A″, cytochrome *c*, and lysozyme with a maximum protein concentration constraint of 1.0 m*M* and a separation gap constraint of 0.5 (Fig. 8d) reveals that the substitution of α-chymotrypsinogen A″ into the feed stream had no effect on the optimum gradient slope. The reason is clear; since both α-chymotrypsinogen A and α-chymotrypsinogen A″ elute first, their nonlinear adsorption behavior has no impact on the gap between the first component and the product. Because the infinite dilution elution time of the first component remains unaffected by the change in steric factor, the optimum gradient slope remains the same.

On the other hand, for a separation of α-chymotrypsinogen A″, cytochrome *c*, and lysozyme with no separation gap constraint (Fig. 11d), there is a significant decrease in gradient slope as compared to the separation of the original feed stream (Fig. 11a). Examination of Fig. 11a reveals that α-chymotrypsinogen A has reached its maximum protein concentration constraint. Thus, the determining factor in selection of the optimum gradient slope in this separation is the concentration of α-chymotrypsinogen A. Since a decrease in the steric factor will result in a more concentrated peak, running the simulation with the same (16 m*M*/column dead volume) gradient slope results in a violation of the maximum protein concentration constraint. To prevent this, the gradient slope must be decreased in the α-chymotrypsinogen A″, cytochrome *c*, and lysozyme separation.

Now consider a change in the nonlinear adsorption behavior of the product. Cytochrome *c*′ has the same linear adsorption parameters as cytochrome *c*; however, its steric factor is half that of cytochrome *c*. As can be seen by comparing Fig. 8a and Fig. 8e, when cytochrome *c*′ replaced cytochrome *c* as the product and a separation gap constraint of 0.5 was included, the optimum gradient slope increased. The separation was more easily carried out because the product formed a narrower band in the final chromatogram. On the other hand, for the corresponding sample displacement separation (Fig. 11e), no effect on the gradient slope was observed as compared to the original feed stream (Fig. 11a). In spite of the change in product steric factor, the concentration of the low affinity impurity remained essentially the same preventing any change in the gradient slope.

Although these results are case specific, they provide qualitative insight into the effect of the equilibrium adsorption properties of the feed components on the optimum gradient slope for both the case of a finite separation gap and the case of sample displacement.

5. Conclusions

Preparative linear gradient chromatography is an inherently nonlinear process. Loading protein under conditions of low salt concentration causes concentration of the protein on the stationary phase and leads to nonlinear adsorption which profoundly effects the observed chromatograms. In this study, it has been seen that a chromatographic model based on Steric Mass Action equilibrium can account for

this nonlinear adsorption and can accurately predict preparative ion-exchange performance.

In this work, issues of feed concentration, the adsorption properties of the feed, feed volume, gradient slope, purity, and product concentration were considered. Other issues remain to be addressed. These include operating pH, choice of stationary phase, choice of eluting salt, selectivity reversal, and the relative concentration of the product in the feed stream. Further, gradient operation must be compared with other modes of nonlinear chromatography in order to gain a broader vision of the effect of all the variables available to preparative chromatographers.

Nevertheless, this work demonstrates that a simple iterative procedure can be employed to establish optimal separation conditions for preparative linear gradient chromatography. The results indicate that a distinctive optimum exists for linear gradient separations when a separation gap constraint is imposed.

Under conditions of high feed load, it is possible to induce sample displacement behavior in these preparative linear gradient systems. In fact, this competitive binding can be employed to dramatically improve the separation productivity. However, in establishing the optimum linear gradient in sample displacement operations, consideration must be given to the concentration of the product stream. Without a realistic physical constraint on concentration, any optimization scheme will likely choose an impractically steep gradient slope.

While preparative linear gradient separations with finite gaps between the peaks are sensitive to the equilibrium properties of the feed components, sample displacement separations are less sensitive, resulting in simplified methods development. Thus, these results indicate that under appropriate conditions, sample displacement can be easily employed to increase the production rate as observed previously by other researchers [31,32]. Clearly, the limits of this "induced sample displacement" behavior must be examined in more detail.

6. List of symbols

C_i	mobile phase concentration (mM)
$C_{i,f}$	feed concentration (mM)
C_{max}	protein concentration constraint (mM)
D_i	effective dispersion coefficient (cm^2/s)
F_i	function which returns Q_i when given C_1, C_2,...C_{NC} (mM)
G_{slope}	gradient slope (mM)
H	height equivalent to a theoretical plate (m)
K_{1i}	equilibrium constant
k'	capacity factor
L	column length (m)
N	theoretical plates per meter (m^{-1})
NC	number of components present in mobile phase
PR_i	production rate (μmol/(ml h))
$\underline{Q_i}$	stationary phase concentration (mM)
Q_1	bound salt which is not sterically shielded (mM)
$\hat{Q}_1$	bound salt which is sterically shielded (mM)
t	time dimension (s)
t_{cyc}	cycle time of a single chromatographic operation (s)
t_0	column dead time (s)
u_0	chromatographic velocity, $u_0=u_s/\epsilon$, (cm/s)
V_{col}	empty column volume (cm^3)
V_f	feed volume (cm^3)
V_{sp}	stationary phase volume, $V_{sp} = (1 - \epsilon)V_{col}$, (cm^3)
X	axial dimension of column (cm)
x	nondimensional length, $x = (X/L)$

6.1. Greek letters

α_{ij}	separation factor
β	phase ratio, $\beta=(1 - \epsilon)/\epsilon$
ϵ	void fraction
Λ	column capacity (mM)
ν_i	characteristic charge
σ_i	steric factor
τ	nondimensional time, $\tau\ (t/t_0) = (V/V_0)$
τ_f	nondimensional feed injection time
τ_{gap}	nondimensional time separating two adjacent peaks
τ_{sep}	nondimensional time from end of injection until product finishes eluting

6.2. Subscripts

i mobile/stationary phase component number ($i=1$ designates salt)

Acknowledgments

This research was funded by Pharmacia Biotech and a Presidential Young Investigator Award to S.M. Cramer from the National Science Foundation.

Appendix

The linear solvent strength theory of Snyder and coworkers [1] allows retention to be predicted in the linear or Henry's law region of a single component isotherm. This theory has found widespread usage [2,3]. For the case of linear gradient chromatography, the retention time of an infinitely dilute peak may be calculated by the following method using the notation of the SMA isotherm. It is assumed that the protein has zero velocity during the loading cycle.

Under dilution conditions with respect to protein concentration, the path of a protein peak may be predicted using the expression:

$$\frac{d\tau}{dx} = 1 + \beta K_{12}\left(\frac{\Lambda}{C_1}\right)^{\nu_2} \tag{A1}$$

where the subscript 1 refers to the salt and the subscript 2 refers to the protein. Substituting the expression for a linear gradient with initial strength at $\tau=0$ of C_0 and slope G concentration units per dimensionless time unit:

$$\frac{d\tau}{dx} = 1 + \beta K_{12}\left(\frac{\Lambda}{C_0 + G(\tau - x)}\right)^{\nu_2} \tag{A2}$$

Now substituting the variable $\tau^*=\tau-x$:

$$\frac{d\tau^*}{dx} = \beta K_{12}\left(\frac{\Lambda}{C_0 + G\tau^*}\right)^{\nu_2} \tag{A3}$$

The integral may be written:

$$\int_0^{\tau^*} (C_0 + G\tau^*)^{\nu_2}\, d\tau^* = \int_0^{x} \beta K_{12}\Lambda^{\nu_2}\, dx \tag{A4}$$

The solution is:

$$\tau^* = \frac{((\nu_2 + 1)G\beta K_{12}\Lambda^{\nu_2}x + C_0^{\nu_2+1})^{\frac{1}{\nu_2+1}} - C_0}{G} \tag{A5}$$

The path of the protein peak may be calculated by substituting x values into eqn. (A5) and calculating the corresponding $\tau=\tau^*+x$ values.

References

[1] L.R. Snyder and M.A. Stadalius, in C. Horváth (Editor), High-Performance Liquid Chromatography—Advances and Perspectives, Vol. 4, Academic Press, New York, 1986, pp. 208–316.
[2] S. Yamamoto, M. Nomura and Y. Sano, AIChE. Journal, 33 (6) (1987) 1426.
[3] E.S. Parente and D.B. Wetlaufer, J. Chromatogr., 333 (1986) 29.
[4] S.J. Gibbs and E.N. Lightfoot, Ind. Eng. Chem. Fund., 25 (1986) 490.
[5] D.D. Frey, Biotechnol. Bioeng., 25 (1990) 1055.
[6] G. Carta and W.B. Stringfield, J. Chromatogr., 605 (1992) 151.
[7] S. Yamamoto, K. Nakanishi, R. Matsuno and T. Kamikubo, Biotechnol. Bioeng., 25 (1983) 1465.
[8] S. Yamamoto, K. Nakanishi, R. Matsuno and T. Kamikubo, Biotechnol. Bioeng., 25 (1983) 1373.
[9] F.D. Antia and C. Horváth, J. Chromatogr., 484 (1989) 1.
[10] L.R. Snyder, J.W. Dolan and G.B. Cox, J. Chromatogr., 540 (1991) 21.
[11] T. Gu, Y. Truei, G. Tsai and G. Tsao, Chem. Eng. Sci., 47 (1992) 253.
[12] J.C. Bellot and J.S. Condoret, J. Chromatogr., 635 (1993) 1.
[13] R.D. Whitley, X. Zhang and N.H.L. Wang, AIChE. Journal, 40 (6) (1994) 1067.
[14] C.A. Brooks and S.M. Cramer, AIChE. Journal, 38 (12) (1992) 1969.
[15] S.R. Gallant, A. Kundu and S.M. Cramer, J. Chromatogr. A, 702 (1995) 125.
[16] N.K. Boardman and S.M. Partridge, Biochem. J., 59 (1955) 543.
[17] F. Helfferich and G. Klein, Multicomponent Chromatography: Theory of Interference, Marcel Dekker, New York, 1970.
[18] R.R. Drager and F.E. Regnier, J. Chromatogr., 359 (1986) 147.
[19] A. Velayudhan and C. Horváth, J. Chromatogr., 443 (1988) 13.
[20] R.D. Whitley, R. Wachter, F. Liu and N.-H.L. Wang, J. Chromatogr., 465 (1989) 137.
[21] Y. Li and N. Pinto, J. Chromatogr., 658 (1994) 445.
[22] A. Velayudhan, Studies in Nonlinear Chromatography, Doctoral Dissertation, Yale University, New Haven, 1990.

[23] S.D. Gadam, G. Jayaraman and S.M. Cramer, J. Chromatogr., 630 (1993) 37.
[24] J.A. Gerstner and S.M. Cramer, Biotechnology Progress, 8 (1992) 540.
[25] J.A. Gerstner and S.M. Cramer, BioPharm., 5 (1992) 42.
[26] G. Jayaraman, S.D. Gadam and S.M. Cramer, J. Chromatogr., 630 (1993) 53.
[27] S.D. Gadam, S.R. Gallant and S.M. Cramer, AIChE. Journal, 41 (7) (1995) 1676.
[28] S.R. Gallant, A. Kundu and S.M. Cramer, Biotech. Bioeng., 47 (1995) 355.
[29] M. Czok and G. Guiochon, Anal. Chem., 62 (1990) 189.
[30] Z. Ma and G. Guiochon, Comput. Chem. Eng., 15 (1991) 415.
[31] G.B. Cox and L.R. Snyder, J. Chromatogr., 590 (1992) 17.
[32] A. Felinger and G. Guiochon, Biotechnol. Bioeng., 41 (1993) 134.